N91-30233

A Theoretical Comparison of the Near-Optimum Design and Predicted Performance of n/p and p/n Indium Phosphide Homojunction Solar Cells

Chandra Goradia, William Thesling
Space Photovoltaic Research Center*, Electrical Engineering Department
Cleveland State University,
Cleveland, Ohio 44115
and
Irving Weinberg
NASA Lewis Research Center, Cleveland, Ohio 44135

ABSTRACT

Using our detailed simulation model of p^+nn^+ and n^+pp^+ Indium Phosphide (InP) homojunction solar cells, we have done extensive parametric variation computer simulation runs to help us arrive at near-optimum designs of these two solar cell configurations. In this paper, we present the values of all the geometrical and material parameters corresponding to the near-optimal designs of both these configurations. Next, for each configuration, we present the results of parametric variation runs showing how the performance parameters J_{sc}, V_{oc} and η vary with each of the cell design parameters for the near-optimally designed cell. Finally, we discuss the theoretical results obtained and compare the relative merits and drawbacks of the two configurations.

INTRODUCTION

In recent years, in laboratory irradiation tests, indium phosphide (InP) homojunction solar cells have shown a markedly higher tolerance to 1 MeV electron and 10 MeV proton irradiation than silicon (Si) and gallium arsenide (GaAs) solar cells [1]; this fact makes indium phosphide solar cells very attractive for space applications [2]. The main task in the design of InP solar cells is, then, to design them as to yield the maximum possible beginning-of-life (BOL) energy conversion efficiency, comparable to, or greater than that obtained from gallium arsenide solar cells (≈22% at AM0, 25°C).

Using a fairly complete computer simulation model of the homojunction InP solar cell [3], we have done an extensive parameter variation study which has allowed us to come up with near-optimum designs of the InP homojunction solar cell in both its n^+pp^+ (n-on-p) and p^+nn^+

*Funded by NASA Lewis Research Center

(p-on-n) configurations. Having obtained the near-optimum designs of the two configurations, we then re-did the parameter variation study such that while each parameter was being varied individually, all other parameters were kept fixed at their near-optimum values. It is the results of such a parameter variation study of the near-optimum cell design that we present in this paper. While so doing we also compare the theoretically predicted performance of near-optimally designed n^+pp^+ (n-on-p) and p^+nn^+ (p-on-n) InP homojunction space solar cell configurations. Such a comparison is necessary and useful since, there is no a priori reason why a particular one of these two configurations should have the higher beginning-of-life (BOL) efficiency. In addition, we had shown in an earlier paper [4], that the primary factor limiting the open circuit voltage and efficiency of the n^+pp^+ InP homojunction solar cell is the relatively large heavy doping factor in the heavily doped p^+ back-surface field (BSF) region and had mentioned there that since the heavy doping factor in heavily doped n-type InP is quite likely much smaller than that in p-type InP, it was worth investigating the BOL performance of the near-optimally designed p^+nn^+ InP solar cell.

RESULTS AND DISCUSSION

A. Near-Optimum Designs

Table 1 gives the geometrical, material and performance parameters of the near-optimum designs of the n^+pp^+ and p^+nn^+ (p-on-n) homojunction InP solar cell configurations. In this table, the values of the minority carrier indirect or Hall-Shockley-Reed lifetime coefficients in n- and p-type InP are assumed to be ten times the values obtained by matching (curve-fitting) the measured curves of illuminated I-V, $\log_{10}I_{sc}$ versus V_{oc} and spectral response, to the corresponding calculated curves, for an n^+pp^+ homojunction InP solar cell made by the Spire Corporation (Cell Spire 6 [5]). This is along the same lines as we have done earlier [4] As indicated in the table, the heavy doping factors in the various regions were also obtained by matching the calculated and measured curves for the above measurements for the Spire 6 solar cell. The minority carrier mobilities and diffusivities in the various regions were obtained in the same manner as we have explained before [3]. The design parameters, namely, the thickness of and doping in each cell region were obtained from an extensive parametric variation study and are those values which yield the maximum efficiency.

In comparing the n^+pp^+ and p^+nn^+ near-optimum cell designs, note the considerable difference in the emitter thickness of the two configurations. Because of the significantly higher electron mobility compared to hole mobility in InP, the minority carrier diffusion length is much longer in p-type InP than in n-type InP. Hence, it is advantageous to have most of the incoming photons be absorbed in the p-type InP, regardless of configuration. This means that the p-region should be as close to the surface as possible and should be wide enough to absorb most of the incoming photons. This is achieved by choosing either the p^+nn^+ configuration with a wide emitter or the n^+pp^+ configuration with a thin emitter. An immediate implication of this fact is that a larger fraction of the short circuit current I_{sc} comes from the emitter in the p^+nn^+ configuration compared to that in the n^+pp^+

Table 1 **Geometrical, Material and Performance Parameters of Near-Optimum n^+pp^+ and p^+nn^+ Homojunction Indium Phosphide Solar Cells.**

a) n^+pp^+ Structure

Grid Shadow	4.0%
Front SRV	1 x 10^4 cm/sec
W_E	200 Å
$N_{D,emitter}$	3 x 10^{18} cm^{-3}
* $HD_E = n_{iE} / n_{i0}$	0.837
* τ_{HSR}	6.667 ns
τ_{Rad}	0.469 ns
$\tau_{p,E}$	0.437 ns
$L_{p,E}$	0.229 µm
W_{base}	4.0 µm
$N_{A,base}$	8 x 10^{15} cm^{-3}
HD_{base}	1.0
* τ_{HSR}	3.750 µs
τ_{Rad}	0.176 µs
$\tau_{n,B}$	0.168 µs
$L_{n,base}$	43.29 µm
W_{BSF}	250 µm
$N_{A,BSF}$	7.5 x 10^{16} cm^{-3}
HD_{BSF}	1.0
* τ_{HSR}	400 ns
τ_{Rad}	18.74 ns
$\tau_{n,BSF}$	17.89 ns
$L_{n,BSF}$	12.45 µm

* Quantities obtained from Spire 6 match.

J_{SC}	= 39.94 mA / cm^2
V_{OC}	= 901.3 mV
J_{max}	= 38.57 mA / cm^2
V_{max}	= 804.4 mV
FF	= 86.21 %
η	= 22.60 %

b) p^+nn^+ Structure

Grid Shadow	4.0%
Front SRV	1 x 10^3 cm/sec
W_E	3500 Å
$N_{A,emitter}$	1 x 10^{18} cm^{-3}
* $HD_E = n_{iE} / n_{i0}$	3.0
* τ_{HSR}	30 ns
τ_{Rad}	1.406 ns
$\tau_{n,E}$	1.327 ns
$L_{n,E}$	2.971 µm
W_{base}	3.0 µm
$N_{D,base}$	1 x 10^{16} cm^{-3}
HD_{base}	1.0
* τ_{HSR}	2.0 µs
τ_{Rad}	140.6 ns
$\tau_{p,B}$	131.3 ns
$L_{p,base}$	7.349 µm
W_{BSF}	300 µm
$N_{D,BSF}$	5.0 x 10^{18} cm^{-3}
HD_{BSF}	1.0
* τ_{HSR}	4.0 ns
τ_{Rad}	0.281 ns
$\tau_{p,BSF}$	0.249 ns
$L_{p,BSF}$	0.152 µm

* Quantities obtained from Spire 6 match.

J_{SC}	= 39.65 mA / cm^2
V_{OC}	= 915.3 mV
J_{max}	= 38.32 mA / cm^2
V_{max}	= 808.5 mV
FF	= 85.35 %
η	= 22.56 %

configuration, as shown in Table II. This table gives, for the n^+pp^+ and p^+nn^+ configurations, the components of the short circuit current density J_{SC} from each of the emitter, space charge and base regions, both in terms of mA/cm^2 and as fractions of the total current density. Note that in the p^+nn^+ configuration, over 92% of the short circuit current I_{SC} comes from the emitter and space charge regions while in the n^+pp^+ configuration, only 30.5% of I_{SC} comes from these regions. This fact has strong implications on the radiation damage in these two configurations. For a radiation environment in which the radiation-induced defect creation in the InP material occurs primarily at a depth ≥ 1 µm, the p^+nn^+ structure will suffer very little degradation of its I_{SC} compared to the n^+pp^+ structure for which about 70% of its I_{SC} comes from deeper in the base region. For a radiation environment in which defect creation in the InP

material occurs close to the surface (≤ 1 μm), the p^+nn^+ structure will suffer more degradation of its I_{sc} than the n^+pp^+ structure.

Table 2 Fractions of I_{sc} coming from various regions of near-optimally designed n/p and p/n solar cells.

	Emitter	SCR	Base	Total
n/p	6.36	5.83	27.74	39.94 mA/cm²
	15.9 %	14.6 %	69.6 %	100 %
p/n	31.6	4.97	3.06	39.65 mA/cm²
	79.7 %	12.5 %	7.72 %	100 %

In comparing the beginning-of-life (BOL) performance of the near-optimum designs of the n^+pp^+ and p^+nn^+ solar cell configurations, we see from Table I that the near-optimum designs of both the n^+pp^+ and p^+nn^+ configurations are capable of yielding essentially the same 1 AM0 25°C efficiency of slightly over 22.5%. The p^+nn^+ configuration has a somewhat higher V_{oc} but somewhat lower J_{sc} and FF than the n^+pp^+ configuration.

B. Parametric Variation Study

1) Front Surface Recombination Velocity S_F.

Figures 1a,b,c show, respectively, the J_{sc}, V_{oc} and η of n^+pp^+ and p^+nn^+ near-optimum InP solar cells as functions of the front surface recombination velocity S_F. Note that all performance parameters, J_{sc}, V_{oc} and η degrade heavily with increasing S_F in the upper ranges of S_F for only the p^+nn^+ configuration. The performance

Fig. 1a Current Density J_{sc} of Near-Optimum Cell vs. front SRV S_F

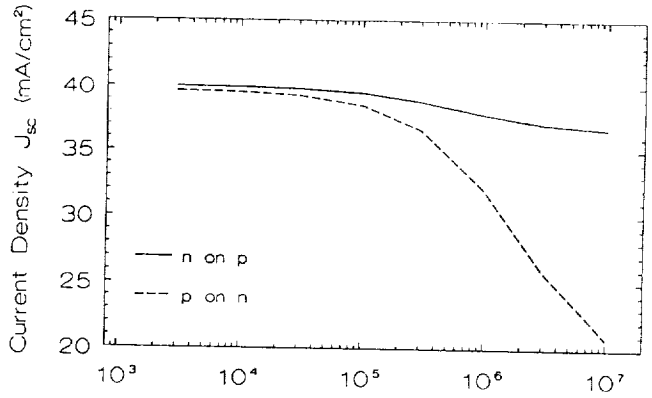

Fig. 1b Open Circuit Voltage of Near-Optimum Cell vs. front SRV S_F

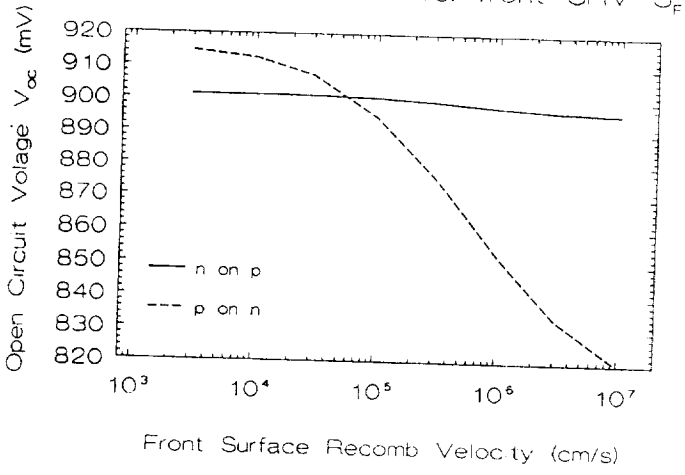

Fig. 1c Efficiency η of Near-Optimum Cell vs. front SRV S_F

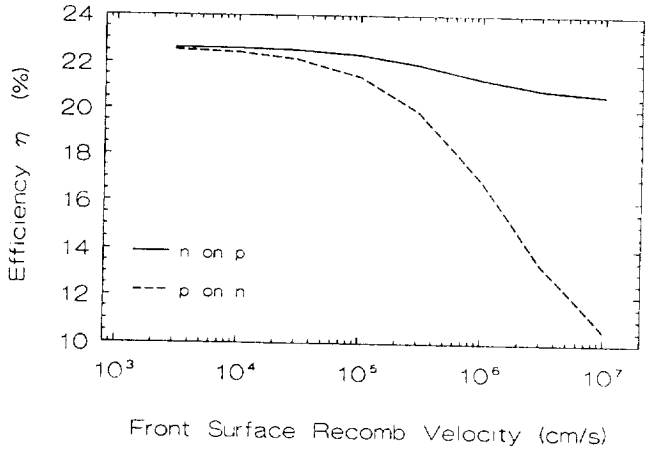

degradation is relatively minor for the n^+pp^+ configuration even at S_F values approaching its limiting value of $v_{th}/2 \sim 10^7$ cm/s. This grossly different dependence on S_F for the n^+pp^+ and p^+nn^+ configurations is easy to explain if we consider that because of its substantially thicker emitter, the p^+nn^+ configuration has most of its photocurrent coming from the emitter and this makes the p^+nn^+ configuration much more sensitive to all the emitter parameters (front SRV, emitter doping, emitter thickness etc.) than the n^+pp^+ configuration.

2) Emitter Thickness W_E.

Fig. 2a Current Density J_{sc} of Near-Optimal cell vs. Emitter Width

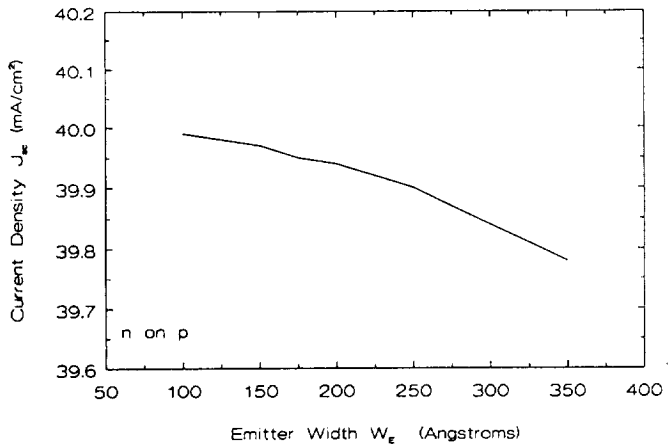

Fig. 2b Current Density J_{sc} of Near-Optimal Cell vs. Emitter Width

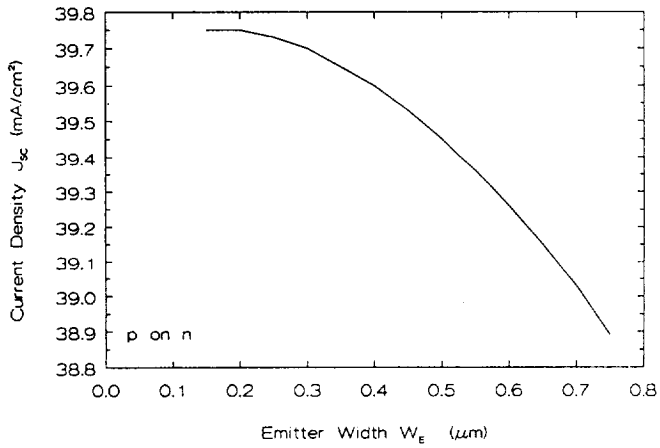

parameters, J_{sc}, V_{oc} and η vary little, less than 2%, as the emitter thickness varies from 100Å to 350Å for the n^+pp^+ and from 0.1 μm to 0.75 μm for the p^+nn^+ configuration. Note also that all the three performance parameters J_{sc}, V_{oc} and η initially increase monotonically as the emitter

Figures 2a,b show, respectively, the J_{sc} for the n^+pp^+ and p^+nn^+ configurations while Figures 2c,d show the V_{oc} and η for the same two configurations, all as functions of the emitter thickness W_E. Here, note that for both the n^+pp^+ and p^+nn^+ configurations, all performance

Fig. 2c Open Circuit Voltage & Efficiency of Near Optimal cell vs. Emitter Width

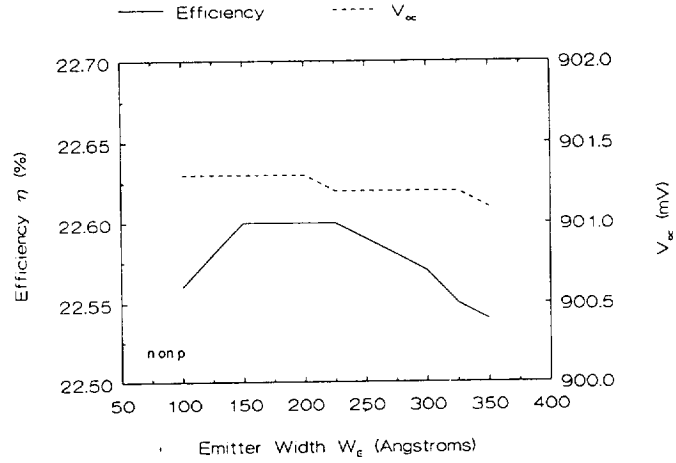

Fig. 2d Open Circuit Voltage & Efficiency of Near Optimal cell vs. Emitter Width

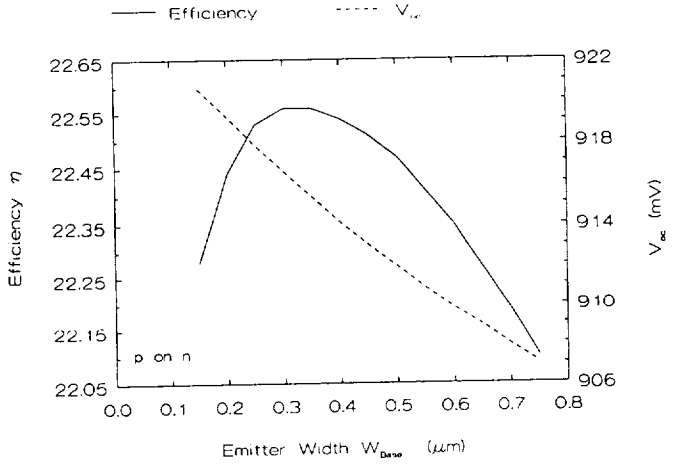

thickness W_E decreases. While this trend holds for J_{sc} and V_{oc} all the way down to W_E = 100Å for the n^+pp^+ configuration and W_E = 0.1μm for the p^+nn^+ structure, the curve for η peaks in the range of W_E between 150Å and 225Å for the n^+pp^+ and W_E between 0.3 and 0.4 μm for the p^+nn^+ structure. For W_E shorter than the lower limits of these ranges, the efficiency η decreases with further decreases in W_E. This is because in these ranges of W_E values, the overall series resistance of the solar cell is dominated by the emitter sheet resistance which increases with decreasing W_E, causing the fill factor FF and thereby also the efficiency η to decrease with decreasing W_E. Thus for both the n^+pp^+ and p^+nn^+ configurations, there is an optimum range of values of W_E, which yield the highest efficiency. For the n^+pp^+ structure this optimum range of W_E is from ~150Å to ~225Å, while for the p^+nn^+ structure, the optimum range of W_E is 0.25-0.425 μm.

Fig. 3a Current Density J_{sc} of Near-Optimum Cell vs. Emitter Doping N_E

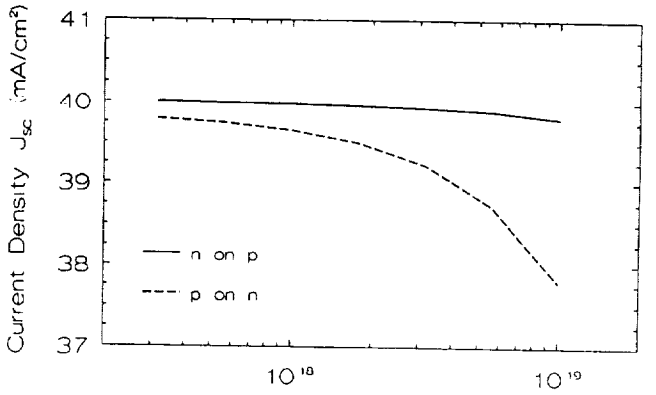

Fig. 3b Open Circuit Voltage of Near Optimum Cell vs. Emitter Doping N_E

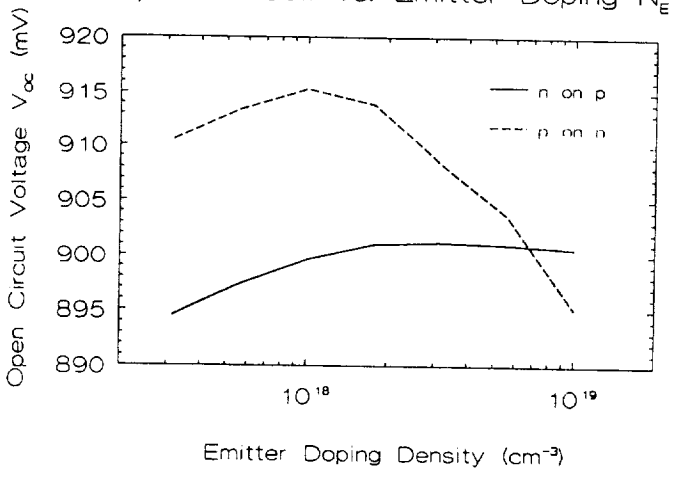

Fig. 3c Efficiency η of Near-Optimum Cell vs. Emitter Doping N_E

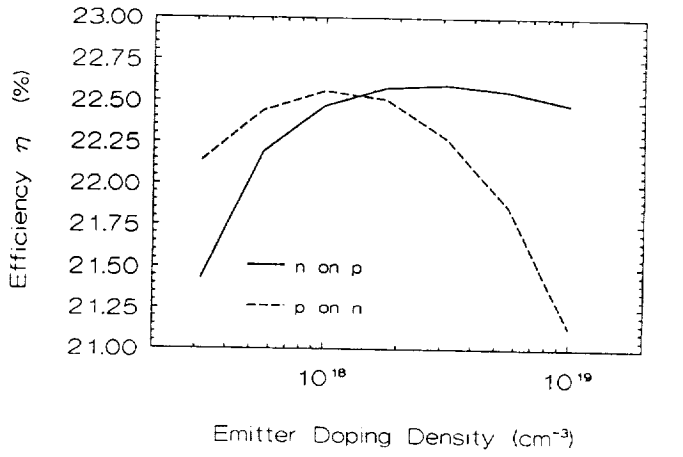

3) Emitter Doping N_{dE} or N_{aE}.

Figures 3a,b,c show, respectively, the J_{sc}, V_{oc} and η of n^+pp^+ and p^+nn^+ near-optimum InP solar cells as functions of the emitter doping concentration N_{dE} or N_{aE}. The calculations for these figures take into account heavy doping effects in the emitter, in the same manner as we have done earlier [4], when the doping there exceeds 10^{17} donor or acceptor atoms per cm^3. As the emitter doping increases from 10^{17} to 10^{19} cm^{-3}, two detrimental effects come into play. First, the radiative lifetime in the emitter decreases in inverse proportionality to the doping increase and secondly, the effective bandgap narrowing significantly increases the effective intrinsic carrier

concentration, thereby increasing the dark saturation or loss current. Of these, it is primarily the first effect, namely, the reduction of lifetime, which is responsible for the degradation of J_{sc} with increased emitter doping. However, both detrimental effects affect V_{oc} and cause it to degrade with increasing doping.

Here, in comparing the n^+pp^+ and p^+nn^+ configurations, we see that the n^+pp^+ cell suffers only a ~0.6% drop in its J_{sc} as the emitter doping increases from 10^{17} to 10^{19} cm^{-3} while the p^+nn^+ cell suffers a 5.12% reduction in its J_{sc} over the same range of emitter doping increase. This difference in behavior is easily explained, knowing that in the p^+nn^+ structure about 80% of the J_{sc} comes from the emitter as compared to only about 16% from the emitter for the n^+pp^+ structure. Thus, as the minority carrier lifetime and diffusion length in the emitter reduce with increased doping in that region, a larger current is affected in the p^+nn^+ structure than in the n^+pp^+ structure, giving a larger amount of degradation in the p^+nn^+ compared to the n^+pp^+ structure.

As to the variation of V_{oc} and η with emitter doping, we see a somewhat different behavior between the n^+pp^+ and p^+nn^+ structures. For the n^+pp^+, both V_{oc} and η first rapidly increase with increasing emitter doping, and then very very gradually decrease with further increases in emitter doping. For the p^+nn^+ cell, V_{oc} first decreases, reaches a minimum at an emitter doping of $3*10^{17}$ cm^{-3}, then increases, reaches a maximum, and then decreases continually up to an emitter doping of 10^{19} cm^{-3}. The observed behavior of V_{oc} versus emitter doping is explainable by considering the fact that in p-type InP, heavy doping causes a substantial increase in n_{ie}, the effective intrinsic carrier concentration, thereby increasing the loss current (dark saturation current) and reducing V_{oc} [4]. In n-type InP, heavy doping causes the bandgap to widen rather than become narrow [4]. Therefore, n_i either reduces or, at worst, stays the same. Thus, for the n^+pp^+ cell, there is no degradation of V_{oc} due to heavy doping effects and the rather slight reduction of V_{oc} with increasing emitter doping seen in Figure 3b is due to the reduction of the minority carrier lifetime in the emitter with increasing doping there. For the p^+nn^+ cell, at emitter dopings higher than ~10^{18} cm^{-3}, V_{oc} decreases with increasing emitter doping due to both, the heavy doping factor and the reduction in lifetime. Hence, a much steeper decline in V_{oc} with increasing emitter doping is seen for the p^+nn^+ structure as compared to the n^+pp^+ structure.

4) Base Width W_B

Figures 4 a,b,c show, respectively, the J_{sc}, V_{oc} and η of n^+pp^+ and p^+nn^+ InP homojunction solar cells as functions of the base thickness W_B. First considering figure 4a, we see that J_{sc} increases monotonically with base thickness for both the n^+pp^+ and p^+nn^+ configurations and substrates at a value of slightly below 40 mA/cm^2 at a base thickness of about 4μm. In this regard, both the n^+pp^+ and p^+nn^+ configurations behave similarly and there is no unexpected behavior anywhere. Figure 4b,c show the V_{oc} and η of the two configurations as functions of the base thickness. In comparing the two configurations with respect to their V_{oc} as a function of base thickness, we note that the n^+pp^+ cell shows V_{oc} initially rising with increasing base thickness, reaching a maximum of about 905 mV at a

Fig. 4a Current Density J_{sc} of Near-Optimum Cell vs. Base Width

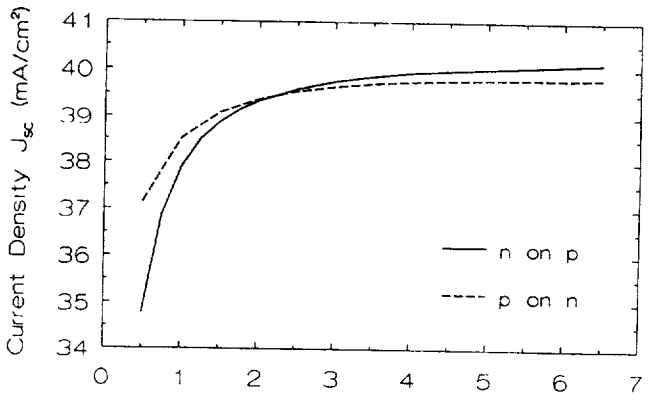

Fig. 4b Open Circuit Voltage of Near-Optimum Cell vs. Base Width

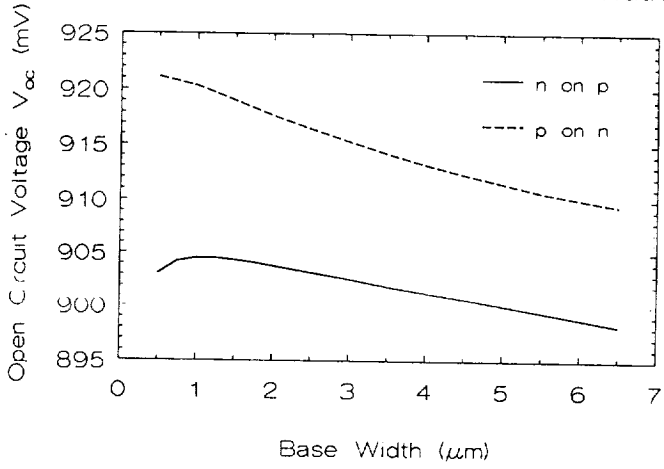

Fig. 4c Efficiency η of Near-Optimum Cell vs. Base Width

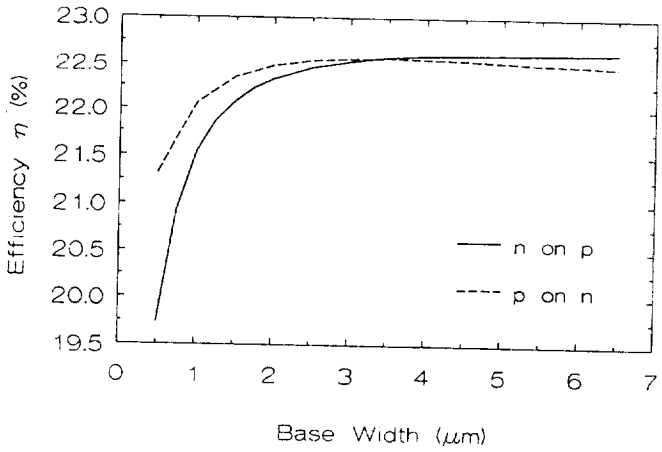

thickness of about 1μm and then falling with increasing base thickness. For the p^+nn^+ configuration, the maximum V_{oc} is about 921 mV and occurs at a base thickness of approximately 0.5μm. As to the variation of efficiency with base width, figure 4c shows η rising rapidly with increasing base thickness, reaching η = 19.7% at W_B = 0.5μm, for the n^+pp^+ cell and η = 21.3% at W_B = 0.5μm for the p^+nn^+ cell. Both configurations saturate to 1AM0, 25°C η of very close to 22.5% for base thickness greater than ~3.5μm.

5) Base Doping N_{aB} or N_{dB}.

Figures 5a,b,c show, respectively, the J_{sc}, V_{oc} and η of n^+pp^+ and p^+nn^+ InP homojunction solar cells as functions of the base doping N_{aB} or N_{dB}. First, considering figure 5a, we see that the J_{sc} of the n^+pp^+ device is slightly but consistently higher than J_{sc} of the p^+nn^+ device. This difference is due to the fact that most of the photogenerated carriers in the p^+nn^+ cell come from the emitter where, because of the heavier doping needed to reduce the sheet resistance to a reasonable value, the minority carrier lifetime is shorter and the collection efficiency of these photogenerated carriers is poorer than in the less heavily doped base region, where most of the photocurrent comes from for the n^+pp^+ cell.

Next, looking at figure 5b, which shows V_{oc} versus base doping, we see that the V_{oc} of the p^+nn^+ near-optimum cell is consistently higher than that of the near-optimum n^+pp^+ cell. This is explainable on the basis that heavy doping effects play a detrimental role only in p-type InP. Then, for the n^+pp^+ structure, the increased recombination in the p^+ BSF

Fig. 5a Current Density J_{sc} of Near-Optimum Cell vs. Base Doping

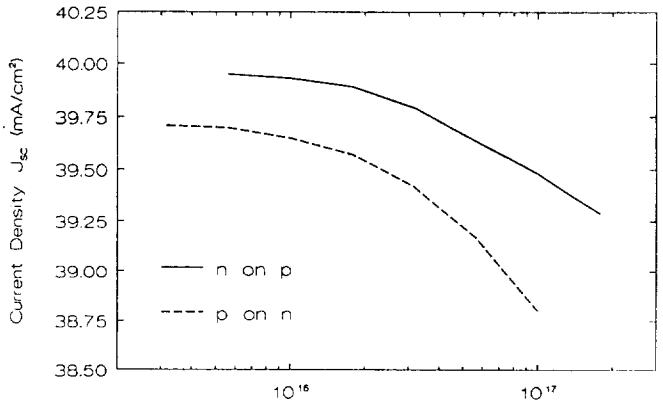

Fig. 5b Open Circuit Voltage of Near-Optimum Cell vs. Base Doping

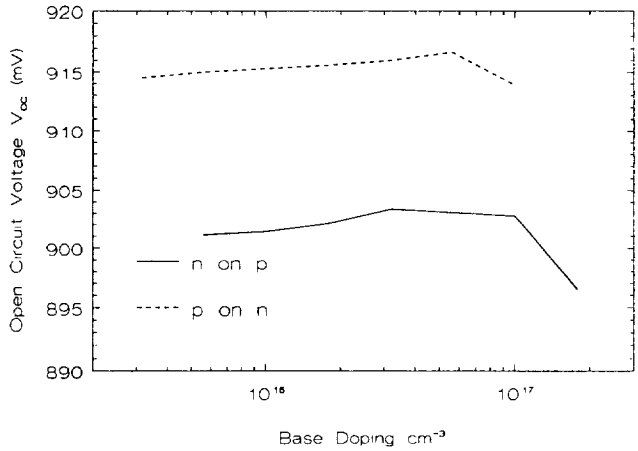

Fig. 5c Efficiency η of Near-Optimum Cell vs. Base Doping

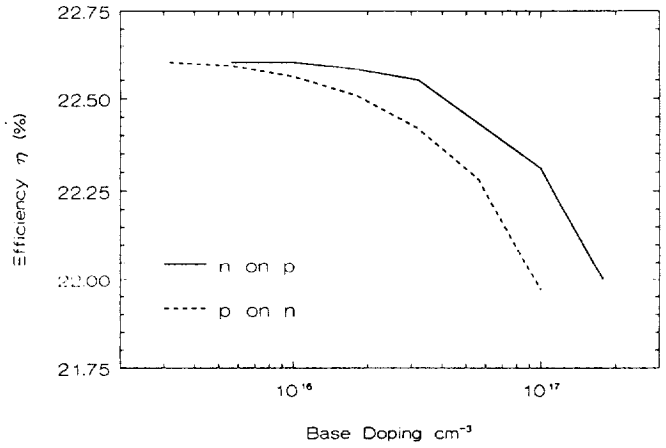

increases the effective SRV at the base/BSF pp^+ interface and increases the dark forward current or loss current component from the base and reduces the V_{oc}. For the p^+nn^+ structure, on the other hand, the increased recombination in the p^+ emitter due to heavy doping effects is not as detrimental in terms of the amount of V_{oc} reduction as is the increased recombination in the p^+ BSF region in the n^+pp^+ structure. This is because of the much smaller volume of the emitter, with its thickness of only 400Å, compared to the volume of the BSF region, with its thickness of $\geq 10\mu m$.

Finally, looking at figure 5c, showing η as a function of base doping for both structures, we see that for a base doping less than ~ $5*10^{15}$ cm^{-3}, both near-optimum structures have the same efficiency of 22.6% at 1AM0, 25°C. However, as the base doping increases, the n^+pp^+ structure starts showing a higher η than the p^+nn^+ structure and the difference in η between the two structures keeps widening with increasing base doping.

CONCLUDING REMARKS

1. From Table 1 as well as the figures showing the efficiency η versus any of the parameters, we see that the near-optimal designs of both the n^+pp^+ and p^+nn^+ InP homojunction solar cell configurations appear capable of yielding beginning-of-life (BOL) 1AM0, 25°C efficiency of slightly over 22.5%. It should be noted that our near-optimum designs use realistically achievable values of 4% grid shadowing, a two-layer AR coating of ZnS/MgF_2, front SRV values of 10^4 cm/s on top of th n^+ emitter

and 10^3 cm/s on top of the p^+ emitter. The thickness of and doping in each region also have realistic values. The primary requirement to achieve the efficiency of 22.5% is that the indirect or Hall-Shockley-Reed minority carrier lifetime coefficients for n-type and p-type InP be ten times their values found from the solar cell Spire6.

With the materials technology of InP constantly improving, we expect this to be achievable in the very near future, if it is already not so.

2. For both the n^+pp^+ and p^+nn^+ configurations, the largest fraction of the photocurrent comes from the p-type region - p^+ emitter in the p^+nn^+ cell and p-type bases in the n^+pp^+ cell. Hence the performance of the cell is most sensitive to the geometrical and material parameters of the p-type region in each configuration.

3. The maximum efficiencies of the two configurations being nearly equal, the choice of configuration (n^+pp^+ or p^+nn^+) is dictated by other considerations such as ease and cost of fabrication and radiation tolerance under a specific radiation environment.

REFERENCES

[1] M. Yamaguchi, C. Uemuer and A. Yamamoto, "Radiation Damage in InP Single Crystals and Solar Cells", J. Appl. Phys., 55 (1984) p. 1429

[2] I. Weinberg, C. K. Swartz, R. E. Hart, Jr., "Potential for use of InP Solar Cells in the Space Radiation Environment", Conf. Rec. 18th IEEE Photovoltaic Specialists Conf., Las Vegas, Oct. 1985, pp. 1722-1724. (See also I. Weinberg, "Indium Phosphide Solar Cells for use in Space", Solar Cells, vol. 29, pp 225-244, 1990.)

[3] C. Goradia, J.V.Geier, I. Weinberg, "Theory of the InP Shallow Homojunction Solar Cell", Solar Cells, vol 25, (1988), pp.235-253

[4] C. Goradia, W. Thesling and I. Weinberg, "Key Factors Limiting the Open Circuit Voltage of n+pp+ InP Solar Cells", Conf. Rec. 21st IEEE Photovoltaic Specialists Conf., Orlando, Fla., May 1990, pp. 386-393

[5] C.J. Keavney, M.B. Spitzer, Appl. Phys. Lett. 52(17) 25 April 1988, pp. 1439-40